Journal of Non-Crystalline Solids 576 (2022) 121245

Contents lists available at ScienceDirect

Journal of Non-Crystalline Solids

journal homepage: www.elsevier.com/locate/jnoncrysol

Relaxation in non-Markovian models: From static to dynamic heterogeneity

C. Torregrosa Cabanilles [*,a], J. Molina-Mateo [a], R. Sabater i Serra [a,b], J.M. Meseguer-Dueñas [a,b], J.L. Gómez Ribelles [a,b]

[a] Center for Biomaterials and Tissue Engineering, Universitat Politècnica de València, València 46022, Spain
[b] CIBER-BBN, Biomedical Research Networking Center in Bioengineering, Biomaterials and Nanomedicine, València 46022, Spain

ARTICLE INFO

Keywords:
Glass transition
Non-Markovian processes
Local potential energy landscape
Relaxation times

ABSTRACT

Glass transition processes have often been explained in terms of wide distributions of relaxation times. By means of a simple stochastic model we here show how dynamic heterogeneity is the key to the emergence of the glass transition. A non-Markovian model representing a small open region of the amorphous material was previously shown to reproduce the time and thermal characteristic behavior of supercooled liquids and glasses. Due to the interaction of the open regions with their environment, the temperature dependence of the equilibrium relaxation times differs from the featureless behavior of the relaxation times of closed regions, whose static disorder does not lead to a glass transition, even with wider distributions of equilibrium relaxation times. The dynamic heterogeneity of the open region produces a glass transition between two different regimes: a faster-than-Arrhenius and non-diverging growth of the supercooled liquid relaxation times and an average Arrhenius behavior of the ideal glass. The Kovacs' expansion gap was studied by evaluating the nonequilibrium distribution of relaxation times after the temperature quenches.

1. Introduction

Condensed matter is typically in a solid state at low temperatures, at which the molecules that form the material have very reduced mobility due to their strong interactions. If the temperature of a solid material is increased sufficiently, the mobility of its components also increases, until it is normally able to flow with greater or lesser viscosity in what is called the liquid state. The transition between both states is performed in different ways depending on the microscopic structure of the solid material. Crystalline solids have an ordered structure that becomes disordered in the solid-to-liquid phase transition at a characteristic melt temperature. However, as the temperature of solids without long range order (glasses) increases, their viscosity progressively decreases by several orders of magnitude, without evident changes in their disordered structure, until the liquid state is reached in a process known as glass transition.

Glasses are metastable systems whose properties depend on their history and evolve over time, with long relaxation times [1–3]. The glass transition temperature can be measured when a liquid is supercooled fast enough from the melting temperature (if this exists). It can also be measured through the response of the system to external oscillating actions, as in dielectric and mechanical spectroscopy. As with many other relaxation techniques, the results are usually interpreted in terms of time or frequency-dependent functions. The exponential function of time $\phi(t) = \exp(-t/\tau)$ and the Debye function of frequency $\widetilde{\phi}(\omega) = (1 + i\omega\tau)^{-1}$, simplest models used, with a unique relaxation time τ, often fail to reproduce experimental results. Different but related empirical functions [4], fitting with a small number of parameters, can also be used.

Experimental results frequently show the time dependence of the observable average value. This information is useful for the study of the system in thermodynamic equilibrium, but may not be enough if the study is extended to out-of-equilibrium states as in glasses, where relaxation time depends on thermal history and not only on the instantaneous state [2]. The glass transition and structural relaxation processes have often been explained in terms of the wide distribution functions $g(\log\tau)$ as a superposition of exponential relaxations,

$$\phi(t) = \int_{-\infty}^{\infty} d\log\tau\, g(\log\tau)\exp(-t/\tau), \tag{1}$$

and susceptibility as a superposition of Debye functions,

* Corresponding author.
E-mail address: ctorregr@fis.upv.es (C. Torregrosa Cabanilles).

https://doi.org/10.1016/j.jnoncrysol.2021.121245
Received 19 January 2021; Received in revised form 5 October 2021; Accepted 18 October 2021

$$\widetilde{\phi}(\omega) = \int_{-\infty}^{\infty} d\log\tau\, g(\log\tau)(1 + i\omega\tau)^{-1}. \quad (2)$$

Mathematically, a Kohlrausch-Williams-Watts function $\phi(t) = \exp(-t/\tau)^{\beta}$, commonly used as an empirical model to describe stretched relaxations, is equivalent to a specific superposition of exponential relaxations. Moleculat dynamics simulation studies [5] have recently shown that the stretching of the relaxation cannot be simply assigned to the superposition of spatially distributed heterogeneities, but already exists on a very local scale.

Obtaining a model-free distribution of relaxation times from experimental data is a difficult task and it has been proposed to describe the distribution of relaxation times by means of logarithmic moments that quantify the characteristic time of the relaxation, its width or stretching, and its asymmetry [6]. Molecular mobility has often been characterized in computer simulations using different approaches to evaluate the distribution of relaxation times in equilibrium states [7,8].

The glass transition process is both non-linear and non-exponential, which leads to very complex behavior including memory effects [9]. A wide variety of phenomenological and stochastic models are used in the glass transition area that reproduce and explain many of its characteristics [10], sometimes with formalisms that include a distribution of relaxation times [11] or a vibrational density of states related to relaxation times [12]. But the fundamentals of the glass transition phenomena and its kinetic or thermodynamic origin are still being discussed [2]. A simple model that adequately reproduces the phenomenology associated with glass transition would be a useful tool to obtain further qualitative and quantitative insights into multiple questions which have been considered for decades [2,3].

Glass-forming materials are characterized by spatial and temporal clusters of fast and slow moving particles [1], leading to the so called dynamical heterogeneity. This heterogeneity is particularly outstanding as the material approaches the glass transition [13–15]. Some regions within the material reduce their mobility, while others exhibit faster dynamics. Over time, these fast and slow regions dynamically change their mobility within the material. Recently, even unsupervised machine learning techniques used to detect the connection between structure and dynamics in glasses identified two populations of particles in molecular dynamics simulations based on a description of their local environments. Their distribution was described by two Gaussians, corresponding to the faster and slower groups of particles in the system [16].

The evolution of a small closed region of a material, made up of a cluster of particles in contact with a thermal bath at a specific temperature, can be considered as a stochastic process whose state changes according to the probability of the transitions between the different energy levels (given by the Arrhenius factor). This is a Markov process related to the potential energy landscape formalism [17].

However, in condensed matter, the strong interaction of each small region with its environment forces the region to be considered as an open system, and its evolution may no longer fulfill the Markov condition. As the system plus environment dynamics is reduced to an effective Markovian description when the coupling is weak [18] in our case it is reduced to a simple non-Markovian model of the region when the coupling is strong. In this case the transitions between the system's states not only depend on the present state but also on the previous states, and non-Markovian dynamics appear. The non-Arrhenius behavior of the viscosity of fragile liquids has recently been shown to be a consequence of the non-Markovian dynamics that characterize these systems' diffusive processes [19].

The authors have already applied non-Markovian models to qualitatively reproduce various characteristic phenomena involved in glass transition [20–22], such as its dependence on cooling rate, the heat capacity step and overshoot peaks, the stretched exponential shape of the structural relaxation and the Kovacs asymmetry and the memory effect. In this paper we use a non-Markovian model to analyse the description of relaxation times in liquid and glass states and the glass transition phenomena. The equilibrium states and their relaxation time distributions are determined in a wide range of temperatures, including glassy states. Both a super-Arrhenius growth of the relaxation times on cooling and the natural emergence of the glass transition temperature are obtained only when the heterogeneous dynamics is set in the model through non-Markovianity. The evaluation of the nonequilibrium states during isothermal relaxations after a quench allowed us to interpret the Kovacs' expansion gap [23–25] within the formalism of the distribution of relaxation times.

2. Non-Markovian model and methodology

The non-Markovian model of a small open cluster of the material has previously been reported by the authors in ref. [22]. The model considers the states and evolution of a homogeneous amorphous material composed of small open regions which interact with their dynamically heterogeneous environment [10,13]. The nanoscale size of the region is small enough so that the number of possible configurations is considerably reduced. These configurations (also known as inherent structures [26,27]) correspond to the energy minima of the so-called local potential energy landscape, which define their energy levels and their intervening barriers [26,28–31].

On one side, the evolution of a closed region can be described by a Markov process, where the probability of the transitions between its different configurations and energy levels depends only on the present configuration. At each discrete time interval or Markov step (MS), the process transition matrix of a closed region from its current energy level j to the following level k happens with transition probabilities

$$w_{jk}(T,h) = \frac{w_0}{n}\exp\left[-\frac{E_{jk}+h}{k_B T}\right] \quad (3)$$

as a thermally activated process with energy barriers given by h, where n is the number of energy levels and $w_0 = 1$, so that the transition rate at very high temperature has been set to $1/n$. $E_{jk} = (E_k - E_j)\theta(E_k - E_j)$ depends on the energy values E_j and E_k of the levels j and k, and θ is the Heaviside step function. The no-transition rate is given by $w_{jj} = 1 - \sum_{k\neq j} w_{jk}$. The state of the system at time t as an ensemble of equivalent regions is described by a vector $d_i(t)$ with the population of every energy level.

On the other side, the non-Markovian dynamics appears in our model when an open region is considered to possess high or low mobility due to the interaction with its environment. This heterogeneity of the dynamics is usually characterized by different parameters such as the softness of a particle [32] or other order parameters depending, for instance, on the particle's trajectory in the space that leads to a dynamic phase transition in atomic models of glass-forming materials [33]. A kinetic lattice model with three-states of mobility sites and nearest-neighbor interactions has been applied to study mobility transport through the fluid [34]. High mobility regions are defined here as those that have just gone through a transition. Conversely, the regions that have not transitioned in the recent past are considered low mobility regions.

Within the non-Markovian model, a region that changed its state on the previous Markov step (classified as a fast region) is characterized by a specific value (h) of the potential barrier height between its inherent structures. And a region that remained in the same state (classified as a slow region) is a scenario with higher potential energy barriers $h' > h$. The effect of the environment on the open region leads to heterogeneous and non-Markovian dynamics, with a different barrier height for its two different mobility alternatives. The second-order transition probability w_{ijk} to a state k therefore depends on the present state j and the previous state i as

$$w_{ijk}(T) = \begin{cases} w_{jk}(T,h) & \text{if } j \neq i \\ w_{jk}(T,h') & \text{if } j = i \end{cases}. \quad (4)$$

The difference between the heigth of the potential barriers' fast and

slow regions can be considered as related to both the strength of the coupling between the region and its environment and the degree of dynamic heterogeneity.

The evolution of the Markov process is calculated in steps, so that the state of the system at the next time step $t+1$ (in MS) is given by

$$d_k(t+1) = \sum_i d_i(t-1) \sum_j d_j(t) w_{ijk} \,, \tag{5}$$

where w_{ijk} is the transition tensor, and $d_j(t)$, $d_i(t-1)$ represent the population vectors of the present and previous states, respectively.

The model satisfies microscopic reversibility in equilibrium according to the detailed balance expression for non-Markovian systems. Consequently, the stationary distribution becomes the equilibrium distribution and our non-Markovian system is an equilibrium system. A detailed study is shown in Appendix A.

As the relaxation time of a simple decay or exponential process is the reciprocal of its rate constant, the relaxation time τ_{ijk} for each process $ij \rightarrow k$ is reciprocally related to the transition probability w_{ijk}. Therefore, the set of relaxation times for a second-order system with n levels is composed of $n^3 - n^2$ terms, pertaining to each possible transition from the states ij to the states $k \neq j$. The list of relaxation times depends on the local potential energy landscape of the cluster (its energy levels and potential barriers) as well as on the temperature. But the distribution of relaxation times also depends on the population of the energy levels. The contribution or weight of a given relaxation time of the transition from a specific level is expected to be proportional to the population of that level.

The distribution of the system's relaxation times from the states given by ij (the previous and present states) depends on $d_i(t-1)d_j(t)$, i.e. the product of the population of the i level of the previous state and the population of the j level of the present state. Therefore each relaxation time is weighted according to the state of the system, and the discrete list of relaxation times and their frequencies can be evaluated and shown as histograms on a logarithmic time scale, with the relaxation times grouped by decades between $\tau_0 = n/w_0 = 10$ MS and 10^{10} MS.

In order to characterize the distribution, the mean relaxation time of the decimal logarithmic distribution $g(\log\tau)$, or characteristic time τ_c, is obtained as the weighted average of $\log\tau$. The width of the distribution, or stretching parameter $\sigma_{\log\tau}$, has also been evaluated as the square root of the variance of the distribution of logarithmic relaxation times, its asymmetry $\gamma_{\log\tau}$ as the skewness of the distribution $g(\log\tau)$, and its kurtosis. These parameters are also good descriptors to compare with the experimental-wide distributions of relaxation times, regardless of the models (see [6]).

For simplicity, the local energy landscape is supposed to lead to $n = 10$ equidistant energy levels between 0 and 1 units of energy. Therefore the discrete distribution of relaxation times of a region in a given state is composed of 900 terms that depend on their intervening energy levels and potential barriers, the temperature and the populations of the energy levels of the previous and present states.

The non-Markovian model is evaluated with three different closed clusters, with potential energy barrier heights $h = h' = 0.1$ (fast closed cluster), $h = h' = 1$ (slow closed cluster), and a 50–50% superposition of both (static mixture). The distributions of relaxation times in equilibrium of these closed clusters, whose potential barriers do not vary and that fulfill the Markov property, are evaluated for comparison with the open clusters.

Three different open clusters are defined with the same value as the fast region's potential barriers $h = 0.1$ and, in each separate case, the specified fixed value of the slow region's potential barriers $h' = 0.2$, 0.5 and 1, representing systems with different degrees of immobility due to their interaction with their environment. Their equilibrium distributions of relaxation times and their response to thermal interactions are calculated and compared with the closed clusters and the glass transition phenomenology using the non-Markovian model implemented in *Mathematica*.

3. Results and discussion

3.1. Distribution of relaxation times at equilibrium

The equilibrium states can be evaluated directly at any temperature as the stationary state of the second-order Markov chain, avoiding the computational cost of evaluating them through the very slow time evolution at low temperatures. Given the values of the parameters that define the transition probabilities, there is a unique equilibrium state and its related distribution of relaxation times in our irreducible and ergodic Markov chain [35], as the limiting probabilities have a unique nonnegative solution.

The distribution of relaxation times of the equilibrium states at different temperatures between $T = 0.1$ and $T = 1$ are shown as histograms for a fast closed region with barrier height $h = 0.1$ (Fig. 1a), a slow closed region with barrier height $h = 1$ (Fig. 1b), and the open region with $h = 0.1$ and $h' = 1$ (Fig. 1c). As the distributions are very broad and vary widely, the logarithmic representation $g(\log\tau)$ is more suitable. The relaxation times are grouped by decades between $\tau_0 = 10^1$ MS and 10^{10} MS.

Interestingly, the distribution of the open region is not a simple o "static" superposition of the distributions of the slow and fast closed regions, but an emergent behavior arises. The equilibrium distribution of the open region is the result of the dynamic disorder [36] of slow and fast regions that depend on the time, as opposed to the static disorder of the closed regions.

The distribution of the relaxation times in the open region shows larger differences than those of a simple superposition of closed regions at the glass transition temperature interval of the open region and below (the glass transition temperature $T_g = 0.17$ was calculated for this system from the cooling sweeps as reported in [22]). This important change of the distributions with temperature can be observed by comparing the histograms at $T = 0.2$ and $T = 0.1$ in Fig. 1c, although it is easier to visualize the transition at the curves showing the descriptors of these distributions versus the inverse of the temperature in Fig. 2b.

The width or standard deviation of the equilibrium distribution of the open region, its asymmetry or skewness and kurtosis clearly show a significant change located around the system's glass transition temperature ($1/T_g \approx 6$). However, the distribution of the closed regions does not have these characteristics and varies monotonously over the entire temperature range (see Fig. 2a). As the shape of the distribution of the closed regions is independent of the value of their potential barriers, the static mixture composed of a 50% of fast closed regions and 50% of slow closed regions does not show any significant transition, in spite of the increased degree of (static) heterogeneity and the increased width of the relaxation time distribution at each temperature.

As temperature decreases, the relaxation time distributions in equilibrium are usually wider in both open and closed regions and their widths are practically inverse of the temperature. A peak appears at the glass transition temperature interval only in the open region, which can be interpreted as an increase of heterogeneity at these temperatures (see Fig. 2b), in good agreement with the increased heterogeneity around T_g of the distribution of accessible volume found in Monte Carlo simulations [37].

3.2. Temperature dependence of the characteristic relaxation time

In order to compare the temperature dependence of the equilibrium relaxation times of the static and dynamically heterogeneous systems, their logarithmic distributions and characteristic values τ_c are shown against $1/T$ at the Arrhenius plots in Fig. 3. The temperature dependence of the relaxation times of the static mixture (Fig. 3a) shows that the only apparent feature is the increased characteristic relaxation time and the

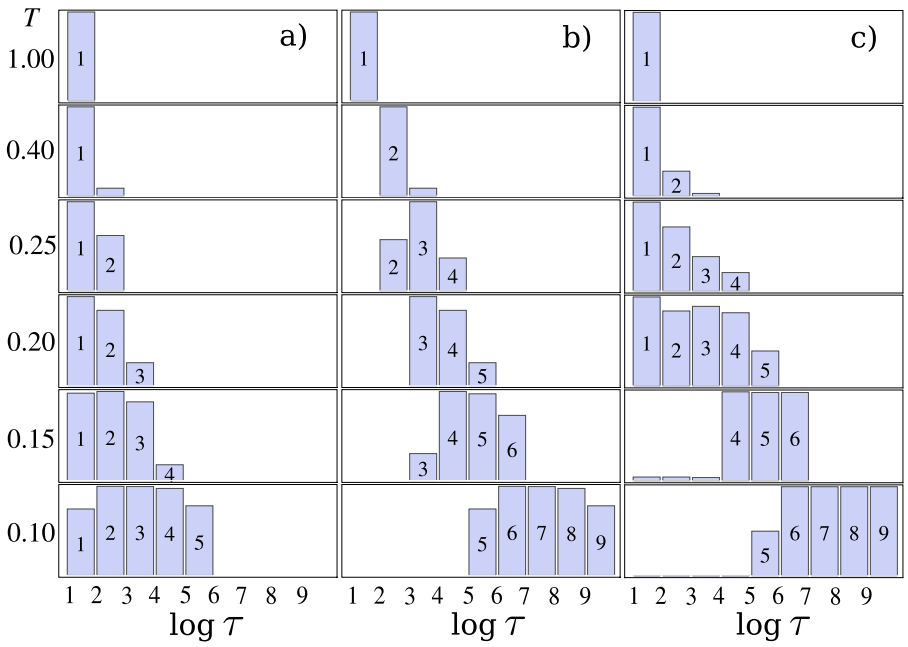

Fig. 1. Distributions of relaxation times of the equilibrium states at different temperatures from 0.1 to 1, for (a) a fast closed region with potential barrier height $h = 0.1$, (b) a slow closed region with potential barrier height $h = 1$ and (c) the open region with potential barriers $h = 0.1$ and $h' = 1$. Every histogram bar (with labels 1 to 9) shows the relaxation times found in a decade from 10^1 MS until 10^{10} MS.

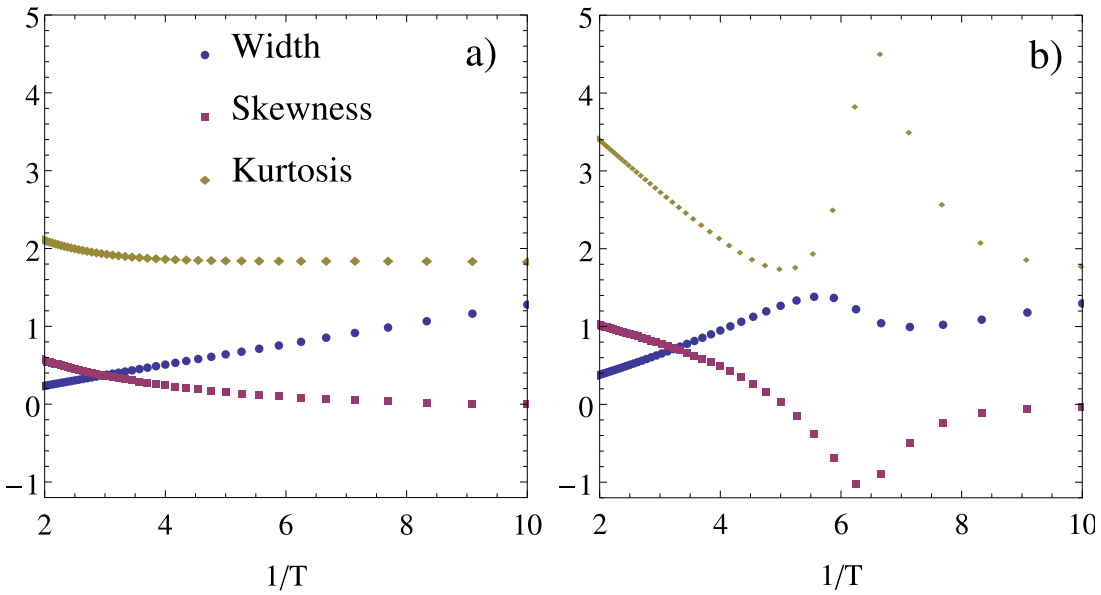

Fig. 2. Moments of the distribution of logarithmic relaxation times, $g(\log\tau)$: width, skewness and kurtosis of the equilibrium distribution according to the reciprocal of the temperature of (a) the closed regions and (b) the open region with potential barrier height $h = 0.1$ and $h' = 1$.

greater width of the distribution when temperature decreases. This Arrhenius dependence is quite obvious since the probability of the transitions increases with temperature as a thermally activated process. The potential energy barrier height is directly related to the constant activation energy of the closed regions.

Nevertheless, the presence of high energy barriers between the energy levels of the open cluster hinders the transitions. This effect is greater for the lower energy levels and at lower temperatures because they are more often slow regions. At higher temperatures the open cluster tends to be faster and the lower barriers predominate, so that a transition appears between the states from low to high temperatures (see Fig. 3b) with several characteristics related to the glass transition.

The faster increase and higher curvature of the relaxation times at temperatures $T > T_g$, than those of the closed region, is related to the change in trend from the predominance of low potential barriers at high temperature to the more likely high potential barriers at lower temperatures. The open region model clearly behaves as expected from the point of view of the potential energy landscape model: “whereas at high temperature the system explores a part of the landscape with low barriers between energy minimums, at lower temperatures it explores minimums with substantially higher energy barriers” [38]. The non-Markovian dynamics of the open region lead to the emergence of a transition around a temperature with glass transition characteristics.

It is interesting to consider this transition from the point of view of

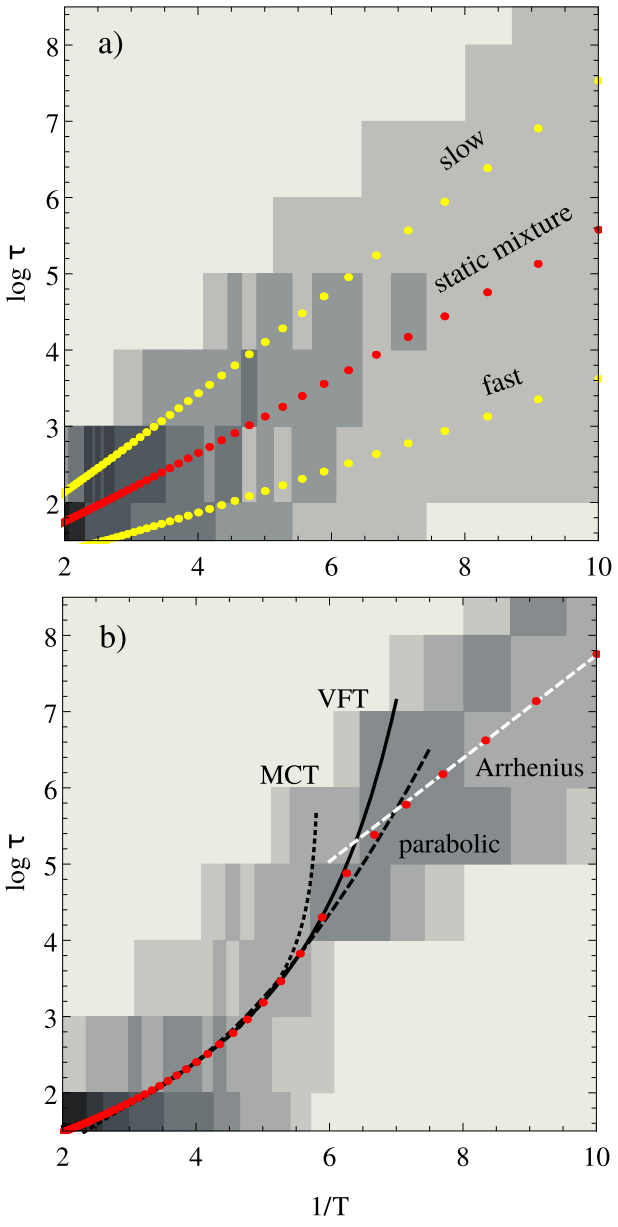

Fig. 3. (a) Equilibrium distribution of relaxation times of the static mixture (darker grey means a higher contribution of the relaxation time at each temperature) according to the reciprocal of temperature. Also shown is the characteristic relaxation time τ_c of the static mixture (red dots), the fast and slow closed regions (yellow dots). (b) Equilibrium distribution of relaxation times of the dynamically heterogeneous open region with potential barriers $h = 0.1$ and $h' = 1$ according to the reciprocal of temperature. Its characteristic relaxation time τ_c (red dots) and the fittings of the supercooled liquid characteristic times to the VFT law (solid line) are also shown, a parabolic law (dashed black line) and the mode-coupling theory dependence (dotted line), as well as the fitting of the glass results to the Arrhenius law (dashed white line). (For interpretation of the references to colour in this figure legend, the reader is referred to the web version of this article.)

Zwanzig's dynamical disorder [36], which usually leads to dynamics with nonexponential decay. When the barrier height of a region is a random function of time it has dynamical disorder, and the evolution of the system involves the entire history of the barrier height. For a given fluctuation time scale t_c of the barrier height, the dynamics depends on the observation time. On one side, for long observation times $t \gg t_c$, the very rapidly fluctuating barriers can be replaced by their time average, and the exponential decay is recovered. On the other side, for short times $t < t_c$, the slowly fluctuating barriers lead to static disorder that may be or not exponential in time. The intermediate cases where the fluctuations are neither slow nor very fast ($t \geq t_c$) are those of dynamical disorder with nonexponential relaxations, in agreement with Ngai's coupling model and the existence of three relaxation regimes [39] if we interpret t_c as the crossover time.

Two other different open regions were compared to study the influence of the height h' of the energy barriers of the slow open region on the results. Both have the same potential energy barriers of the high mobility regions ($h = 0.1$) but lower energy barriers of the low mobility regions ($h' = 0.5$ and 0.2) corresponding to lower dynamic heterogeneity. The results also qualitatively showed the same dependence of the relaxation times on temperature, but with lower curvature and lower values of the glass transition temperature and glass activation energy (see Table 1). As recently pointed out in [19], here we show that a non-Markovian glass transition model leads to non-Arrhenius behavior in the supercooled regime, with a fragility dependent on the potential barriers that represent the interaction of the open region with its environment.

The steepness of the relaxation time curve against $1/T$, related with the Angell concept of fragility [40]

$$m = \left[\frac{\partial \log\tau}{\partial(T_g/T)}\right]_{T=T_g} \tag{6}$$

takes its maximum values around the glass transition temperature and is also a measure of the curvature or departure from Arrhenius behavior. The fragility values of the different open clusters are shown in Table 1 as a function of h', the slow region barrier height. These values are not directly comparable with the experimentally determined fragility values. A very strong real system with an Arrhenius behavior has a fragility around $m = \log\tau(T_g) - \log\tau_0 = 16$. The time scale (in MS) of our model corresponds to $\log\tau_0 = 1$ and the characteristic relaxation time at the glass transition temperature lies around 10^5 MS, so that a fragility parameter $m = 4$ was found for a very strong material. The fragility index $I = m/C - 1$ [41] may be a better parameter for comparing systems with a different relaxation time range $C = \log\tau(T_g) - \log\tau_0$.

Fragility clearly increases with the height of the barriers of the slow region, from a stronger behavior with $h' = 0.2$ and 0.5 to a more fragile system with $h' = 1$. Taking into account that these barriers are related to the blocking produced by the intermolecular interactions (or packing effects) and the intramolecular torsional barriers in polymers, our result is in qualitative agreement with [42], in which a steeper interatomic repulsion leads to more fragile liquids (our model does not yet take thermal expansion into account) and also with the increased polymer fragility with the strength of the intramolecular barriers [43].

The results of the characteristic relaxation time τ_c above T_g are compared with different relaxation models of supercooled liquids in Fig. 3b. In particular, we consider the Vogel-Fulcher-Tamman (VFT) form, the parabolic form Elmatad et al. [44], and the mode-coupling theory (MCT) dependence [45] of the relaxation time with temperature given, respectively, by

Table 1
Values of the parameters of the open cluster with different high barrier heights h', including fitting parameters to the VFT, parabolic and mode-coupling theory relaxation time relations, fragility, activation energy of the glassy states and the glass transition temperature evaluated from the energy evolution curve during a slow cooling sweep, as reported in [22].

h'	T_0	B	T_{on}	J	T_c	γ	m	E_a	T_g
1.0	0.11	0.19	0.7	0.37	0.17	1.8	9.9	1.6	0.17
0.5	0.075	0.19	∞	0.23	0.14	1.8	4.8	1.1	0.14
0.2	0.035	0.20	∞	0.17	0.09	2.0	4.1	0.8	0.09

$$\log\left(\frac{\tau}{\tau_0}\right)_{\mathrm{VFT}} = \frac{B}{T - T_0}, \tag{7}$$

$$\log\left(\frac{\tau}{\tau_0}\right)_{\mathrm{par}} = J^2\left(\frac{1}{T} - \frac{1}{T_{on}}\right)^2, \tag{8}$$

$$\left(\frac{\tau}{\tau_0}\right)_{\mathrm{MCT}} = |T - T_c|^{-\gamma}, \tag{9}$$

where we allow τ_0, B, T_0, J, T_{on}, γ and T_c to be free parameters. Although all the fittings with 3 free parameters are good (see also Fig. 3b), those of the VFT equation are performed with only two free parameters, keeping $\tau_0 = 10$ MS fixed. This value is related to the transition rate $w_0/n = 0.1$ MS^{-1} to any state of our system at a very high temperature. As expected, the results in Table 1 show that the Vogel temperature T_0 is lower for stronger glasses, and closer to T_g in a fragile glass.

The parabolic equation, found empirically and in kinetically constrained models [44], has no singular behavior at any finite temperature. The results of the fitting show (Table 1) that the values of the onset temperature T_{on} for slow dynamics (at which the relaxation behavior moves over from an Arrhenius to a super-Arrhenius form) are very high. The slow dynamics play a role in our model even at high temperatures. The values of J (related to the energy required to generate particle mobility) scale with the glass activation energy, E_a.

The fitting to the MCT expression within its range of validity is performed on a smaller subset of data, at temperatures between $1.2T_g$ and a higher value at which the system does not show double relaxation. Surprisingly, the critical temperature T_c, at which relaxation times diverge with a power law with the exponent γ, is found to be equal to the glass transition temperature in every case. The exponent remains between 1.8 and 2 for systems with different fragility. Our results do not show a divergence at T_g, but it is known that MCT breaks down close to the experimental glass transition temperature. Nevertheless, the critical temperature is usually found above T_g, so that its coincidence in this case is striking.

Below the glass transition temperature, our results deviate both from the MCT and the VFT diverging models. The characteristic relaxation time is closer to the parabolic curve close below T_g. At lower temperatures, the longer of the relaxation times in the distributions roughly follow the parabolic relation, but the distributions are widening and the characteristic relaxation time changes its trend to an Arrhenius behavior with an average constant activation energy E_a, similar to the behavior of the slow close region. Nevertheless, the equilibrium state of the glass and its relaxation times are those of the ideal glass, the limit states after a sufficiently long period of time. They can be close but different to the glassy states attained experimentally.

Deviations from the diverging VFT behavior of the relaxation time have been proposed [46,47]. Results obtained in polymers [47,48] and molecular liquids [49] and in very long aging time experiments as a way of equilibrating glasses below Tg [50] show that relaxation in glasses deviates from the VFT expression towards an Arrhenius-like behavior. In cases where the dynamics roughly depend on the characteristic relaxation time, our model clearly deviates from the VFT model at temperatures below T_g, showing an Arrhenius behavior, in good agreement with the experimental results found with thermally stimulated recovery, creep and dynamic mechanical analysis [51,52].

The long term aging behavior of different polymeric glass formers has shown a double decay of the enthalpy until complete recovery [53], with two time scales with different behavior. Both the shorter relaxation times, with an Arrhenius temperature dependence and small activation energy, and the longer relaxation times, with a temperature dependence typical of the α relaxation, are qualitatively compatible with a distribution of relaxation times as shown at Fig. 3b. The distribution of the open region near and below the glass transition temperature shows the existence of slower and faster processes that diverge on lowering the temperature and merge around T_g. A specific study focused on the distributions of relaxation times at temperatures below T_g will be carried out in future work.

3.3. Isothermal evolution and the expansion gap

Simulations of isothermal relaxations at different temperatures have been performed as examples of the evaluation of the distribution of relaxation times in nonequilibrium states with the non-Markovian model. These simulations can measure the energy and the distribution of relaxation times of the states during the evolution towards the equilibrium after temperature jumps. The fractional energy deviation from equilibrium, $\delta_E = [E(t) - E_\infty]/E_\infty$, where E_∞ is the equilibrium value, is used to describe the energy evolution. The equilibrium state and its energy are evaluated directly at any temperature as the stationary state of the second-order Markov chain, avoiding the computational cost of evaluating it through very slow evolution at low temperatures and a possibly related uncertainty on the evaluation of δ_E.

The asymmetry of the isothermal approach to equilibrium at a given temperature after temperature jumps from higher and lower temperatures (down- and up-jumps, respectively) is a classical glass transition signature [9]. The non-exponential and asymmetric evolution of the energy deviation is a consequence of a complex time evolution of the distribution of relaxation times towards the equilibrium distribution. This evolution has been often characterized by the effective relaxation time τ_{eff}, a measure obtained from the energy relaxation curves as

$$\tau_{eff}^{-1} = -\frac{1}{\delta_E}\frac{d\delta_E}{dt}. \tag{10}$$

The evolution of τ_{eff} leads to characteristic phenomena, such as the Kovacs' expansion gap found in these single-jump experiments [9]. The effective relaxation time at a given temperature does not seem to converge to a single limiting value in the final equilibrium state for different jumps when plotted against δ_E, which is the expansion gap, also known as the τ_{eff} paradox.

The isothermal evolution of the energy deviation δ_E at $T = 0.18$, after a quench from different temperatures $T \pm \Delta T$ with $\Delta T = \pm 0.01$, 0.02, 0.03, 0.04 and 0.05, is shown in Fig. 4a. The results from the non-Markovian model show that, as expected, the fractional deviation of energy approaches zero more slowly in up-jumps than in down-jumps, but these differences in behavior are maintained even for very long times (see inset in Fig. 4a). In those states, whose energy is very close to the equilibrium value, the relaxation process still continues. At these very long times, the energy deviation is very small but the effective relaxation time still depends on the initial state, leading to the slope at origin of the effective relaxation time versus the energy deviation plot (Fig. 4b). The measured gap will depend on the resolution of the δ_E values, which in our model are available at any required resolution. Additionally, as shown at the inset of Fig. 4b, the values of τ_{eff} are very sensitive to the precision of E_∞. Even a deviation lower than 1% produces a false wider gap.

As our model predicts a unique equilibrium state and its related distribution of relaxation times at each temperature, it is only possible to find a unique characteristic relaxation time as a result and therefore only an apparent expansion gap paradox. The expansion gap can be analyzed in terms of the distribution of relaxation times. Figure 4c and d show the evolution of the distribution of relaxation times at $T = 0.18$ after the temperature up-jump from $T = 0.13$ and the down-jump from $T = 0.23$, respectively. The evolution after the up-jump starts with longer relaxation times, leading to a slower evolution towards equilibrium than the down-jump, where the opposite is true. At $t = 100$ MS, it can be seen that the down-jump distribution is very close to the equilibrium, but the up-jump distribution is not that close until $t = 500$ MS is reached.

Previous studies of the volume and enthalpy relaxation that lead to the expansion gap have suggested that its magnitude disappears as the

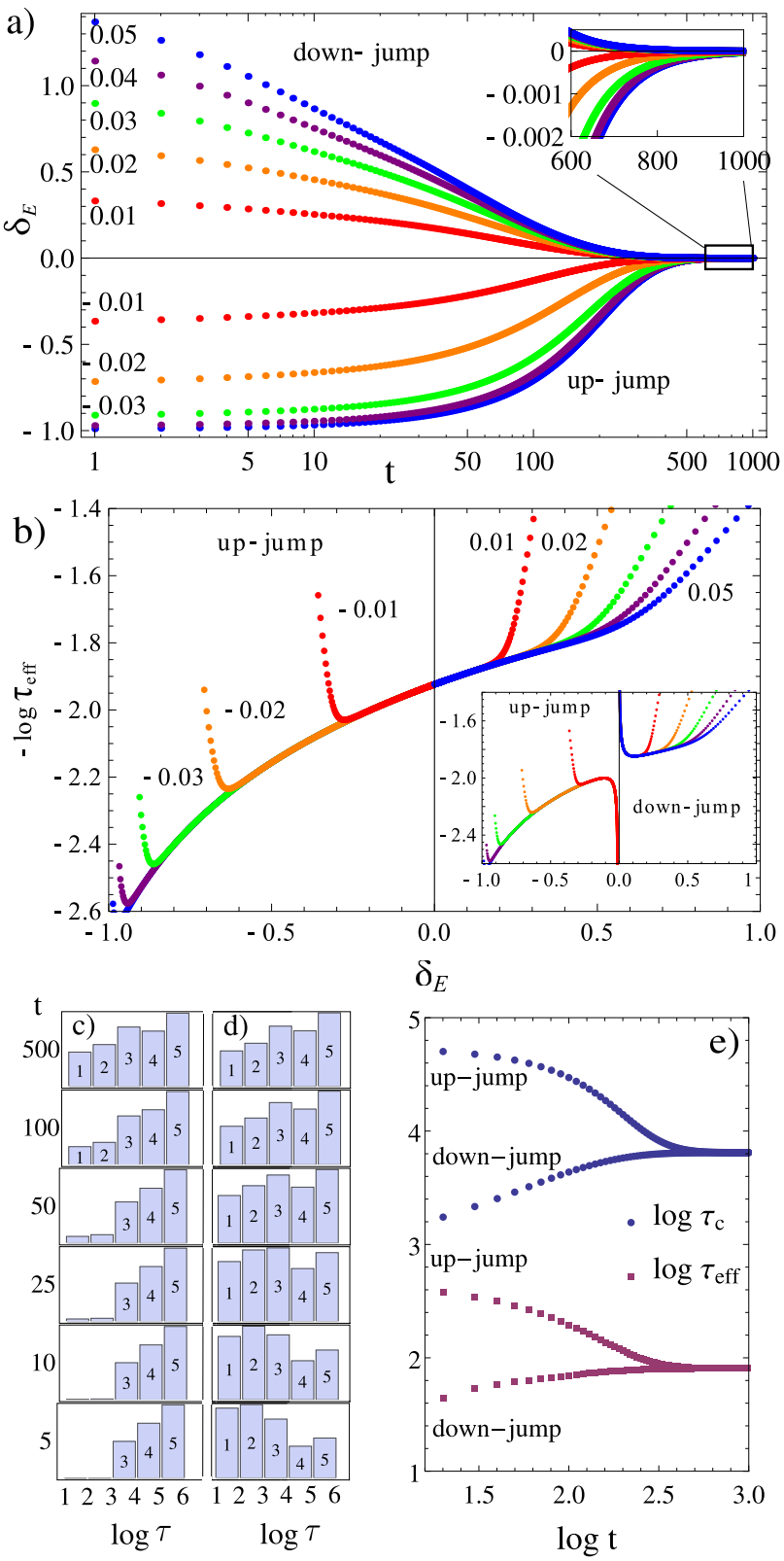

Fig. 4. (a) Isothermal evolution of the fractional deviation of energy at $T = 0.18$ after jumps from $T \pm \Delta T$ in a logarithmic time scale. The inset shows a zoomed selected region in a linear time scale. (b) Effective relaxation time versus the energy deviation. The inset shows the same plot obtained with a slightly higher limit energy E_∞ value (less than 1% higher). The histograms show the distribution of relaxation times during the isothermal evolution at $T = 0.18$ after the up-jump (c) and down-jump (d) from $T \mp 0.05$. (e) Evolution of the characteristic relaxation time τ_c and effective relaxation time τ_{eff} after the same up- and down-jump.

departure from equilibrium approaches zero [23–25]. Nevertheless this phenomenon is important because it seems to be related to the stochastic fluctuations and a strong material memory in glasses, which only stochastic and lattice models have reproduced [25].

The effective relaxation time τ_{eff} is related to the characteristic relaxation time τ_c, as both are different descriptors of the same distribution of relaxation times. Figure 4e shows the evolution of both magnitudes after the up- and down-jumps. The values of τ_c are at least one order of magnitude higher than τ_{eff}, and show a slower convergence towards the equilibrium value than τ_{eff}, showing that the energy evolution depends strongly on the faster relaxation times, although the system state evolution persists over a longer period of time, even when

its energy is very close to the equilibrium value. This difference in time scales has been pointed out as the origin of the apparent expansion gap paradox as explained by McKenna in [23]: "it may be that the expansion gap is merely a manifestation of the longest relaxation time processes occurring in the polymer glass". The interpretation of the asymmetry and the expansion gap in terms of the distributions of relaxation times is also in qualitative agreement with recent lattice simulations [25] where the heterogeneous dynamics of mobile and immobile domains are shown to explain the asymmetry. In that study, the mobile domains displayed a much slower evolution in the up-jump case, consistent with the slow growth of the shorter relaxation times of the up-jump distributions shown in Fig. 4c. It seems that the expansion gap reflects the lack of the shorter relaxation-time processes in the up-jump experiment.

4. Conclusions

The evaluation of the relaxation time distributions in equilibrium and nonequilibrium states by means of a simple non-Markovian model has been shown to be a useful tool for the study of the complex phenomena related to glass-forming materials. This non-Markovian model can reproduce the time evolution and thermal behavior related to glass transition.

The results show that although glass transition is related to wide distributions of relaxation times, it only emerges in our model if dynamic heterogeneity is present. A wide distribution of relaxation times with static disorder, as in the case of the closed cluster, is not enough. Within this model, the glass transition is caused by the dynamic disorder. As a consequence of the interaction of each open region of the material with its environment, the potential energy barriers between its different inherent structures are changing, and its dynamics switch between fast and slow mobility. The results show complex thermal and time behavior, in which a transition between two different regimes emerges that resembles the characteristic behavior of liquid and glass states.

Specific and reproducible results of the model have been presented: according to the current models, the distributions of relaxation times in equilibrium reproduce the non-Arrhenius behavior of the liquid state with different degrees of fragility. At lower temperatures, there is no divergence in the relaxation times and there is a transition towards an average Arrhenius behavior for the ideal glass. Nevertheless, further studies should be conducted on the distribution of relaxation times at these low temperatures beyond its average behavior.

It has also been shown that the non-Markovian model and its interpretation through the distribution of relaxation times can explain issues such as the expansion gap. It has been shown how the different time scales of the relaxation of the system's state on one side, and its energy on the other, cause a faster convergence of the energy towards its equilibrium value than the relaxation times towards the equilibrium distribution. The deficit of short relaxation times in up-jumps significantly contributes to explaining the asymmetry and expansion gap phenomena.

Although the model presented is quite simple, with a local potential energy landscape of a few equidistant energy levels as a harmonic oscillator, and with identical intervening energy barriers, it can be adapted to more complex systems using the energy values and barriers of the potential energy landscape of a cluster or small region of specific material. At the same time the model can be customized to amorphous systems with different values of fragility and T_g and it can be extended, for instance, to include pressure effects. The development of non-Markovian models for specific materials, beyond the toy model used here, can offer interesting results to compare with experimental results.

CRediT authorship contribution statement

C. Torregrosa Cabanilles: Methodology, Formal analysis, Writing – original draft, Writing – review & editing. **J. Molina-Mateo:** Investigation, Software, Formal analysis, Writing – original draft, Writing – review & editing. **R. Sabater i Serra:** Funding acquisition, Supervision, Writing – review & editing. **J.M. Meseguer-Dueñas:** Investigation, Formal analysis, Writing – original draft. **J.L. Gómez Ribelles:** Conceptualization, Formal analysis, Funding acquisition, Supervision, Writing – original draft, Writing – review & editing.

Declaration of Competing Interest

The authors declare that they have no known competing financial interests or personal relationships that could have appeared to influence the work reported in this paper.

Acknowledgement

Funding for open access charge: CRUE-Universitat Politècnica de València. RSS and JMM acknowledge the Spanish Ministry of Science, Innovations and Universities through the RTI2018-097862-B-C21 Project (including the FEDER financial support). CIBER-BBN is an initiative funded by the VI National R&D&I Plan 2008-2011, Iniciativa Ingenio 2010, Consolider Program. CIBER Actions are financed by the Instituto de Salud Carlos III with assistance from the European Regional Development Fund.

Appendix A. Detailed balance

The second-order Markovian model used in this paper conforms to detailed balance, as the system is time symmetrical and it fulfills the equilibrium condition of a non-Markovian system, that can be defined as in ref. [54]:

$$w_{ijk}\,\pi_{ij} = w_{kji}\,\pi_{kj}\,, \tag{A.1}$$

where w_{ijk} is the second-order transition probability from the states ij (previous and current) to the states jk (current and next), and π_{ij} is the distribution of the states ij (previous and current).

In order to prove that our model satisfies the condition of detailed balance for second-order Markov systems (Eq. (A.1)) and the system is reversible in equilibrium, we must find a potential function V so that

$$w_{ijk}\exp[-V(i,j)] = w_{kji}\exp[-V(k,j)]\,, \tag{A.2}$$

in analogy with the condition of detailed balance for a Markov chain (p. 23 in ref. [55]).

We can find a potential V solving Eq. (A.2) by evaluating, according to our model (Eqs. (3) and (4)), the quocient:

$$\frac{w_{ijk}}{w_{kji}} = \frac{A\exp\left[-\beta\left(E_{jk}+h+(h^{'}-h)\delta_{ij}\right)\right]}{A\exp\left[-\beta\left(E_{ji}+h+(h^{'}-h)\delta_{kj}\right)\right]} = \frac{\exp\left[-\beta\left(E_{jk}+(h-h^{'})\delta_{kj}\right)\right]}{\exp\left[-\beta\left(E_{ji}+(h-h^{'})\delta_{ij}\right)\right]} = \frac{\exp[-V(k,j)]}{\exp[-V(i,j)]}\,, \tag{A.3}$$

where δ_{ij} is the Kronecker delta, and $\beta = 1/k_B T$.

So the potential in our model is:

$$V(i,j) = \beta\left(E_{ji} + (h - h')\delta_{ij}\right), \tag{A.4}$$

and $\pi = \exp(-V)$ is the equilibrium distribution of our non-Markovian system.

References

[1] G. Biroli, J.P. Garrahan, Perspective: the glass transition, J. Chem. Phys. 138 (138) (2013) 12A301, https://doi.org/10.1063/1.4795539.

[2] G.B. McKenna, S.L. Simon, 50th Anniversary perspective : challenges in the dynamics and kinetics of glass-forming polymers, Macromolecules 50 (17) (2017) 6333–6361, https://doi.org/10.1021/acs.macromol.7b01014.

[3] K. Niss, T. Hecksher, Perspective: searching for simplicity rather than universality in glass-forming liquids, J. Chem. Phys. 149 (23) (2018) 230901, https://doi.org/10.1063/1.5048093.

[4] F. Alvarez, A. Alegría, J. Colmenero, Relationship between the time-domain Kohlrausch-Williams-Watts and frequency-domain Havriliak-Negami relaxation functions, Phys. Rev. B 44 (14) (1991) 7306–7312, https://doi.org/10.1103/PhysRevB.44.7306.

[5] B. Shang, J. Rottler, P. Guan, J.L. Barrat, Local versus global stretched mechanical response in a supercooled liquid near the glass transition, Phys. Rev. Lett. 122 (10) (2019) 105501, https://doi.org/10.1103/PhysRevLett.122.105501.

[6] R. Zorn, Logarithmic moments of relaxation time distributions, J. Chem. Phys. 116 (8) (2002) 3204–3209, https://doi.org/10.1063/1.1446035.

[7] K. Binder (Ed.), Monte Carlo and Molecular Dynamics Simulations in Polymer Science, Oxford University Press, 1995.

[8] J. Molina-Mateo, J.M. Meseguer Dueñas, J.L. Gómez Ribelles, C. Torregrosa Cabanilles, The distribution of the relaxation times as seen by bond fluctuation model, Polymer 50 (23) (2009) 5618–5622, https://doi.org/10.1016/j.polymer.2009.09.039.

[9] A. Kovacs, Transition vitreuse dans les polymeres amorphes: etude phenomenologique, Fortschritte Der Hochpolymeren-Forschung 3 (1964) 394–507, https://doi.org/10.1007/bfb0050366.

[10] L. Berthier, G. Biroli, Theoretical perspective on the glass transition and amorphous materials, Rev. Mod. Phys. 83 (2) (2011) 587–645, https://doi.org/10.1103/RevModPhys.83.587.

[11] A.J. Kovacs, J.J. Aklonis, J.M. Hutchinson, A.R. Ramos, Isobaric volume and enthalpy recovery of glasses. II. A transparent multiparameter theory, J. Polym. Sci. 17 (7) (1979) 1097–1162, https://doi.org/10.1002/pol.1979.180170701.

[12] A. Zaccone, Relaxation and vibrational properties in metal alloys and other disordered systems, J. Phys. Condens. Matter 32 (20) (2020) 203001, https://doi.org/10.1088/1361-648X/ab6e41.

[13] M.D. Ediger, Spatially heterogeneous dynamics in supercooled liquids, Annu. Rev. Phys. Chem. 51 (1) (2000) 99–128, https://doi.org/10.1146/annurev.physchem.51.1.99.

[14] R. Richert, Heterogeneous dynamics in liquids: fluctuations in space and time, J. Phys. Condens. Matter 14 (23) (2002) 201, https://doi.org/10.1088/0953-8984/14/23/201.

[15] L. Wang, N. Xu, W.H. Wang, P. Guan, Revealing the link between structural relaxation and dynamic heterogeneity in glass-forming liquids, Phys. Rev. Lett. 120 (12) (2018) 125502, https://doi.org/10.1103/PhysRevLett.120.125502.

[16] E. Boattini, S. Marín-Aguilar, S. Mitra, G. Foffi, F. Smallenburg, L. Filion, Autonomously revealing hidden local structures in supercooled liquids, Nat. Commun. 11 (2020) 5479, https://doi.org/10.1038/s41467-020-19286-8.

[17] P.K. Gupta, W. Kob, Basis glass states: new insights from the potential energy landscape, J. Non-Cryst. Solids X 3 (2019) 100031, https://doi.org/10.1016/j.nocx.2019.100031.

[18] J.P. Garrahan, Aspects of non-equilibrium in classical and quantum systems: slow relaxation and glasses, dynamical large deviations, quantum non-ergodicity, and open quantum dynamics, Physica A 504 (2018) 130–154, https://doi.org/10.1016/j.physa.2017.12.149.

[19] A.C. Rosa, C. Cruz, W.S. Santana, E. Brito, M.A. Moret, Non-arrhenius behavior and fragile-to-strong transition of glass-forming liquids, Phys. Rev. E 101 (4) (2020) 42131, https://doi.org/10.1103/PhysRevE.101.042131.

[20] C. Torregrosa Cabanilles, J.M. Meseguer Dueñas, J.L. Gómez Ribelles, J. Molina-Mateo, Cooperativity in the conformational rearrangements of polymer chain segments as seen by bond fluctuation model, Macromol. Theory Simul. 18 (6) (2009) 355–362, https://doi.org/10.1002/mats.200900008.

[21] C. Torregrosa Cabanilles, J. Molina-Mateo, J. Meseguer Dueñas, J. Gómez Ribelles, A simple model for cooperative and non-exponential processes in non-crystalline polymers, J. Non Cryst. Solids 357 (2) (2011) 367–370, https://doi.org/10.1016/j.jnoncrysol.2010.06.040.

[22] C. Torregrosa Cabanilles, J. Molina-Mateo, R. Sabater i Serra, J.M. Meseguer-Dueñas, J.L. Gómez Ribelles, Non-Markovian methods in glass transition, Polymers 12 (9) (2020) 1997, https://doi.org/10.3390/POLYM12091997.

[23] G.B. McKenna, M.G. Vangel, A.L. Rukhin, S.D. Leigh, B. Lotz, C. Straupe, The τ-effective paradox revisited: an extended analysis of Kovacs' volume recovery data on poly(vinyl acetate), Polymer 40 (18) (1999) 5183–5205, https://doi.org/10.1016/S0032-3861(98)00668-5.

[24] S. Kolla, S.L. Simon, The τ-effective paradox: new measurements towards a resolution, Polymer 46 (3) (2005) 733–739, https://doi.org/10.1016/j.polymer.2004.11.086.

[25] M. Lulli, C.S. Lee, H.Y. Deng, C.T. Yip, C.H. Lam, Spatial heterogeneities in structural temperature cause Kovacs' expansion gap paradox in aging of glasses, Phys. Rev. Lett. 124 (9) (2020) 95501, https://doi.org/10.1103/PhysRevLett.124.095501.

[26] F.H. Stillinger, A topographic view of supercooled liquids and glass formation, Science 267 (5206) (1995) 1935–1939, https://doi.org/10.1126/science.267.5206.1935.

[27] A. Heuer, Exploring the potential energy landscape of glass-forming systems: from inherent structures via metabasins to macroscopic transport, J. Phys.: Condens. Matter 20 (37) (2008) 373101, https://doi.org/10.1088/0953-8984/20/37/373101.

[28] M. Goldstein, Viscous liquids and the glass transition: a potential energy barrier picture, J. Chem. Phys. 51 (9) (1969) 3728–3739, https://doi.org/10.1063/1.1672587.

[29] A. Heuer, Properties of a glass-forming system as derived from its potential energy landscape, Phys. Rev. Lett. 78 (21) (1997) 4051–4054, https://doi.org/10.1103/PhysRevLett.78.4051.

[30] T. Iwashita, T. Egami, Local energy landscape in a simple liquid, Phys. Rev. E 90 (5) (2014) 052307, https://doi.org/10.1103/PhysRevE.90.052307.

[31] Y. Fan, T. Iwashita, T. Egami, Energy landscape-driven non-equilibrium evolution of inherent structure in disordered material, Nat. Commun. 8 (2017) 15417, https://doi.org/10.1038/ncomms15417.

[32] E.D. Cubuk, R.J.S. Ivancic, S.S. Schoenholz, D.J. Strickland, A. Basu, Z.S. Davidson, J. Fontaine, J.L. Hor, Y.-R. Huang, Y. Jiang, N.C. Keim, K.D. Koshigan, J.A. Lefever, T. Liu, X.-G. Ma, D.J. Magagnosc, E. Morrow, C.P. Ortiz, J.M. Rieser, A. Shavit, T. Still, Y. Xu, Y. Zhang, K.N. Nordstrom, P.E. Arratia, R.W. Carpick, D.J. Durian, Z. Fakhraai, D.J. Jerolmack, D. Lee, J. Li, R. Riggleman, K.T. Turner, A.G. Yodh, D. S. Gianola, A.J. Liu, Structure-property relationships from universal signatures of plasticity in disordered solids, Science 358 (2017) 1033–1037, https://doi.org/10.1126/science.aai8830.

[33] L.O. Hedges, R.L. Jack, J.P. Garrahan, D. Chandler, Dynamic order-disorder in atomistic models of structural glass formers, Science 323 (5919) (2009) 1309–1313, https://doi.org/10.1126/science.1166665.

[34] N.B. Tito, J.E.G. Lipson, S.T. Milner, Lattice model of mobility at interfaces: free surfaces, substrates, and bilayers, Soft Matter 9 (39) (2013) 9403–9413, https://doi.org/10.1039/c3sm51287h.

[35] S.M. Ross, Markov Chains, 10th ed., Academic Press, 2010.

[36] R. Zwanzig, Rate processes with dynamical disorder, Acc. Chem. Res. 23 (1990) 148–152, https://doi.org/10.1021/ar00173a005.

[37] C. Torregrosa Cabanilles, J. Molina-Mateo, R. Sabater i Serra, J.M. Meseguer-Dueñas, J.L. Gómez Ribelles, Fluctuations of conformational mobility of macromolecules around the glass transition, Phys. Rev. E 97 (6) (2018) 062605, https://doi.org/10.1103/PhysRevE.97.062605.

[38] S. Sastry, P.G. Debenedetti, F.H. Stillinger, Signatures of distinct dynamical regimes in the energy landscape of a glass-forming liquid, Nature 393 (1998) 554–557, https://doi.org/10.1038/31189.

[39] K.L. Ngai, R.W. Rendell, Basic physics of the coupling model: direct experimental evidences, ACS Symp. Ser. 676 (1997) 45–66, https://doi.org/10.1021/bk-1997-0676.ch004.

[40] C.A. Angell, Relaxation in liquids, polymers and plastic crystals - strong/fragile patterns and problems, J. Non Cryst. Solids 131–133 (PART 1) (1991) 13–31, https://doi.org/10.1016/0022-3093(91)90266-9.

[41] J.C. Dyre, N.B. Olsen, Landscape equivalent of the shoving model, Phys. Rev. E 69 (4) (2004) 042501, https://doi.org/10.1103/PhysRevE.69.042501.

[42] J. Krausser, A.E. Lagogianni, K. Samwer, A. Zaccone, Disentangling interatomic repulsion and anharmonicity in the viscosity and fragility of glasses, Phys. Rev. B 95 (10) (2017) 104203, https://doi.org/10.1103/PhysRevB.95.104203.

[43] J. Colmenero, Are polymers standard glass-forming systems? the role of intramolecular barriers on the glass-transition phenomena of glass-forming polymers, J. Phys. Condens. Matter 27 (2015) 103101, https://doi.org/10.1088/0953-8984/27/10/103101.

[44] Y.S. Elmatad, D. Chandler, J.P. Garrahan, Corresponding states of structural glass formers, J. Phys. Chem. B 113 (16) (2009) 5563–5567, https://doi.org/10.1021/jp810362g.

[45] W. Götze, The essentials of the mode-coupling theory for glassy dynamics, Condens. Matter Phys. 1 (4) (1998) 873–904.

[46] I. Avramov, A. Milchev, Effect of disorder on diffusion and viscosity in condensed systems, J. Non Cryst. Solids 104 (1988) 253–260.

[47] J.L. Gómez Ribelles, A. Vidaurre Garayo, J.M. Cowie, R. Ferguson, S. Harris, I. J. McEwen, The length of cooperativity at the glass transition in poly(vinyl acetate) from the modeling of the structural relaxation process, Polymer 40 (1) (1998) 183–192, https://doi.org/10.1016/S0032-3861(98)00213-4.

[48] P.A. O'Connell, G.B. McKenna, Arrhenius-type temperature dependence of the segmental relaxation below Tg, J. Chem. Phys. 110 (22) (1999) 11054–11060, https://doi.org/10.1063/1.479046.
[49] T. Hecksher, A.I. Nielsen, N.B. Olsen, J.C. Dyre, Little evidence for dynamic divergences in ultraviscous molecular liquids, Nat. Phys. 4 (9) (2008) 737–741, https://doi.org/10.1038/nphys1033.
[50] J. Zhao, S.L. Simon, G.B. McKenna, Using 20-million-year-old amber to test the super-Arrhenius behaviour of glass-forming systems, Nat. Commun. 4 (2013) 1–6, https://doi.org/10.1038/ncomms2809.
[51] N.M. Alves, J.F. Mano, J.L. Ribelles, Structural relaxation in a polyester thermoset as seen by thermally stimulated recovery, Polymer 42 (9) (2001) 4173–4180, https://doi.org/10.1016/S0032-3861(00)00552-8.
[52] N.M. Alves, J.F. Mano, J.L. Gómez Ribelles, J.A. Gómez Tejedor, Departure from the Vogel behaviour in the glass transition - thermally stimulated recovery, creep and dynamic mechanical analysis studies, Polymer 45 (3) (2004) 1007–1017, https://doi.org/10.1016/j.polymer.2003.04.002.
[53] D. Cangialosi, V.M. Boucher, A. Alegría, J. Colmenero, Direct evidence of two equilibration mechanisms in glassy polymers, Phys. Rev. Lett. 111 (9) (2013) 095701, https://doi.org/10.1103/PhysRevLett.111.095701.
[54] Q. Zeng, J. Wang, Non-Markovian nonequilibrium information dynamics, Phys. Rev. E 98 (2018) 032123, https://doi.org/10.1103/PhysRevE.98.032123.
[55] C. Maes, An introduction to the theory of Markov processes mostly for physics students, 2016, (Not published).